*Desalination and Water Treatment*
www.deswater.com

doi:10.5004/dwt.2019.23313

141 (2019) 197–207
February

# Kinetics, isotherms, and mechanism of Cr(VI) adsorption by polyaniline/sunflower stem pith composite adsorbent

Xiangyao Liu*, Baohui Wang, Guolin Jing, Ying Qiao

*Chemistry and Chemical Engineering School, Northeast Petroleum University, Daqing 163318, China, Tel.+8613945985500, Fax +86045186609649, email: liuxiangyao1@126.com (X. Liu), wangbaohui60@163.com (B. Wang), jglhgd@163.com (G. Jing), 919479373@qq.com (Y. Qiao)*

Received 27 November 2017; Accepted 19 October 2018

**ABSTRACT**

In the present study, a polyaniline/sunflower stem pith (PANI/SSP) composite was synthesized using in situ polymerization and used as an adsorbent for the detoxification of Cr(VI) from sewage. The work involved batch experiments to investigate the effect of operating parameters such as contact time, pH, temperature, adsorbent dosage, and initial concentration of Cr(VI) on the extent of adsorption by PANI/SSP. The composite was characterized by ATR-FTIR, SEM, TEM, TG-DTG, and XPS. The adsorption process followed the Langmuir isotherm model, and the calculated saturated adsorption amounts obtained from the model ranged from 27.73 to 42.96 mg/g with temperature increasing from 298 to 338 K. Kinetic studies demonstrated that the pseudo second order model is able to provide a realistic description of the adsorption kinetics. A thermodynamic analysis indicated that the removal of Cr(VI) by PANI/SSP is endothermic ($\Delta H^O$ = 37.38 KJ/mol). The regenerated PANI/SSP can be reused successfully for four successive adsorption-desorption cycles. Hence, we conclude that PANI/SSP can be used as an adsorbent for the detoxification of Cr(VI)-contaminated water.

*Keywords:* Polyaniline/sunflower stem pith composite; Hexavalent chromium; Langmuir model; Pseudo second order model

## 1. Introduction

Chromium is a heavy metal pollutant that is a serious threat to humans due to its mobility and persistence in nature. It is primarily present in effluents produced by electroplating, leather tanning, steel fabrication, and the metal finishing industry [1]. In the environment, it is present in two forms, namely, hexavalent chromium and trivalent chromium, where the toxicity of Cr(VI) is 500 times higher than that of Cr(III) [2]. Therefore, several countries across the world strictly control the emission of Cr(VI).

There are some traditional physicochemical treatment methods for the removal of Cr(VI) such as ion exchange, chemical precipitation, membrane separation, and adsorption. Among these methods, adsorption is the most effective and versatile method for the detoxification of Cr(VI) due to its simplicity, its low operating cost, and the abundance of adsorbent. The selection of adsorbent is a key factor in the adsorption of Cr(VI) [3], a widely sourced, environmentally friendly adsorption material with low cost was our first choice.

Biomass materials such as boiled sunflower stems and heads [4,5], coconut coir [6], sawdust [7], and litchi peel waste [8] have attracted intense attention because of their potential novel detoxification of Cr(VI). However, there are still several problems associated with the process such as low removal capacity and slow kinetics; therefore, cellulose fiber should be modified further to enhance their adsorption capacity for Cr(VI).

Polyaniline, a conductive polymer, could have wide applications as the reductant of Cr(VI) due to its low cost and great stability, as doped polyaniline can remove Cr(VI) through an ion exchange reaction. However, one of the disadvantages of polyaniline is its poor process ability. To address this issue, researchers developed composites of polyaniline and porous materials with high specific areas. The polyaniline/mesoporous material hybrid is being

*Corresponding author.

widely investigated for the detoxification of Cr(VI) from sewage through synergistic adsorption and reduction, for instance, there are reported cases of using polyaniline/magnetic mesoporous carbon hybrid [9], polyaniline/magnetic mesoporous silica [10], and other materials.

Sunflower (*Helianthus annuus* L.) is an important oilseed crop. Sunflower stems are present in farming and forestry residues, and the most common disposal method for sunflower stems is incineration; however, this method causes serious air pollution. The sunflower stem pith (SSP), a natural porous material, is well known to have a large specific surface area; hence, the combination of SSP and polyaniline could not only effectively improve the processability of the polyaniline but also add value to SSP by reducing the pollution caused by incineration.

Based on the presented premise, our research team conducted in situ polymerization for preparing polyaniline/sunflower stem pith (PANI/SSP) composites for the detoxification of Cr(VI)-contaminated water using ammonium persulfate (APS) as an oxidant. To better understand the mechanism of using adsorption for Cr(VI) removal, we investigated the adsorption isotherms, kinetic models, thermodynamic parameters, and the effects of other parameters such as the initial concentration of Cr(VI), pH, dosage of fiber composite materials, and reaction times. The results suggest that PANI/SSP is an ideal candidate for the detoxification of Cr(VI) from sewage.

## 2. Materials and methods

### 2.1. Materials

Sunflower stems were collected from the agricultural fields of a village in Zhaoyuan County (China). The SSP was separated from the bark, continuously washed with distilled water to remove impurities and dried thereafter in sunlight until all the moisture was evaporated. Finally, the SSP was cut into 1.5 cm pieces for use. Analytical-grade aniline was freshly distilled under reduced pressure (0.1 MPa) and then stored in a refrigerator at 4°C prior to use. All other chemicals, including APS, hydrochloric acid, sodium hydroxide, and potassium dichromate, were of analytical grade and used without further purification.

### 2.2. Preparation of PANI/SSP

The APS was dissolved in hydrogen chloride solution and then added to a three-neck round-bottom flask with a 1 L capacity for presoaking SSP (6 g on a dry-weight basis); the time allowed for dispersion was 20 min. Aniline was added to the reaction system under continuous stirring (350 rpm) to initiate the polymerization reaction. After a specific reaction time, the in situ polymerization was stopped, and the mixture was filtered. Subsequently, the PANI/SSP was sufficiently washed to remove any unreacted chemicals and then conditioned at room temperature for at least one night.

The optimum process conditions were obtained by single-factor experiments and determined to be a reaction temperature of 298 K, an ammonium persulfate/aniline molar ratio of 1.5 mol/mol, a hydrogen chloride concentration of 1 mol/L, a reaction time of 2 h, an aniline dosage of 4 g/L, and an SSP concentration of 0.6 wt%.

The amount of PANI coated on SSP was calculated according to Eq. (1),

$$\text{PANI coated (\%)} = [(W_2 - W_1)/W_1]\cdot 100 \quad (1)$$

where $W_1$ and $W_2$ are oven-dry weights of the SSP before and after PANI deposition, respectively.

### 2.3. Batch adsorption experiments

First, 100 mL of 100–700 mg/L Cr(VI) at pH values ranging from 1 to 13 was added to Erlenmeyer flasks containing 0.2 g–1 g of PANI/SSP, where the initial pH values of the solution were adjusted using 0.1 mol/L HCl or NaOH. The Erlenmeyer flask was capped and placed in an orbital shaker for 10–60 min, and the residual concentration was analyzed by a UV-Vis spectrometer at 540 nm using 1,5-diphenylcarbazide reagent.

### 2.4. Determination of chromium concentration

The concentration of Cr(VI) was determined by the modified diphenylcarbohydrazide spectrophotometric method (Chinese standard method: GB7467-87) [11]. A standard working curve ($y = 1.3402\ x + 0.00122\ y$) was obtained with a correlation coefficient of 0.9998. To determine the total Cr concentration of the treated water, the water was oxidized by APS for 10 min under acidic and boiling conditions, and then the total Cr concentration was measured according to the same procedure as for the Cr(VI) determination described above. The Cr(III) concentration was calculated from the difference between the total Cr and Cr(VI) concentrations [12].

### 2.5. Kinetic studies

In kinetic studies, the effect of temperature was investigated. PANI/SSP (1.0 g over dry) was brought into contact with 100 mL of a 400 mg/L Cr(VI) solution stirred at 350 rpm at a specified temperature (298 K, 318 K, and 338 K). At preselected times (10, 20, 30, 40, 50, and 60 min), the samples were collected from their three-neck round-bottom flask and filtered through speed filter paper, and the chromium concentrations of the resulting clear filtrate solutions were analyzed. The pseudo first order, pseudo second order, and Elovich models were employed to fit the above experimental data to find the kinetic models that best described the mechanism of adsorption.

### 2.6. Adsorption isotherm

Adsorption isotherm studies were performed at three different temperatures (298 K, 318 K, and 338 K) by agitating 1 g (over dry) of PANI/SSP with 100 mL of Cr(VI) solution of a desired concentration in a 250 mL Erlenmeyer flask on an orbital shaker for 1 h. Thereafter, the samples were collected from the Erlenmeyer flasks and filtered through fast filter paper, and the chromium concentrations of the clear filtrate solutions were analyzed. The equilibrium sorption capacity ($q_e$) of the PANI/SSP was calculated using Eq. (2)

$$q_e = \left(\frac{C_0 - C_e}{m}\right)V \quad (2)$$

where $m$ is the mass of PANI/SSP (g) and $V$ is the volume of solution (L).

The Langmuir, Freundlich, and Temkin adsorption isotherm models were used to fit the above experimental data to determine the adsorption isotherm models that best described the Cr(VI) removal process using PANI/SSP as an adsorbent.

### 2.7. Adsorption thermodynamics

Adsorption thermodynamic studies were performed at five different temperatures (298 K, 308 K, 318 K, 328 K, and 338 K) by agitating 1 g (over dry) of PANI/SSP with 100 mL of a Cr(VI) solution containing 400 mg/L Cr(VI) concentration in a 250 mL Erlenmeyer flask on an orbital shaker for 1 h. Thereafter, the samples were collected from the Erlenmeyer flasks and filtered through speed filter paper, and the concentration of Cr(VI) in the filtrate was analyzed. The $q_e$ was calculated using Eq. (2). The obtained data were fitted with a series of thermodynamic equations to obtain thermodynamic parameters.

### 2.8. Characterization of SSP and PANI/SSP

The morphology and functional groups of SSP and PANI/SSP before and after Cr(VI) adsorption were determined by scanning electron microscopy (SEM) (Sigma, Zeiss Co., Germany) and Tensor 27 Fourier transform infrared (FTIR) spectra (Bruker Co., Germany), respectively. The adsorption mechanism of Cr(VI) was investigated using PHI5700 X-ray photo electron spectroscopy (XPS) with an AI K X-ray source (ULVCA-PHI Co., USA). The Brunauer-Emmett-Teller (BET) specific surface area, pore volume, and pore size distribution of SSP and PANI/SSP before and after Cr(VI) adsorption were measured by an ASAP 2020 surface area and porosity analyzer (Micromeritics Instrument Co., USA). Thermogravimetric (TG)-differential TG (DTG) analysis of the PANI/SSP was carried out with a TG 209 F3 thermogravimetric analyzer (NETZSCH Co., Germany). Transmission electron microscopy (TEM) images of the samples were taken using a JEM-2100 microscope (JEOL Co., Japan)

### 2.9. Desorption studies

Initial adsorption studies were conducted incubating 1 g of the PANI/SSP and 100 mL of 500 mg/L Cr(VI) solution for 6 h at room temperature. Cr ions loaded on PANI/SSP in 0.01 mol/L NaOH solution were desorbed while shaking on an orbital shaker for 40 min at room temperature, and then the solution was filtered through speed filter paper. At the end of the adsorption-desorption experiment, PANI/SSP was treated with 1 mol/L $H_2SO_4$ for the desorption of Cr(III). Thereafter, the PANI/SSP was washed with distilled water, dried at 100°C and subsequently tested for five consecutive adsorption-desorption cycles.

## 3 Results and discussion

### 3.1. Effect of pH

In the adsorption of Cr(VI) using PANI/SSP as adsorbent, solution pH plays a vital role: on one hand, it affects the species of the chromium ion [13], while on the other hand, it not only affects the reducing ability of the polyaniline deposited on the surface of the SSP but also influences the electric charge density on the surface of PANI/SSP and thus impacts the capacity to adsorb Cr(VI) and Cr(III).

In the present study, the effect of the initial pH of the solution on the capacity of PANI/SSP to adsorb Cr(VI), Cr(III) and total Cr was investigated in the initial pH range of 1–13. As shown in Fig. 1A, in the initial pH range from 1 to 5, the concentration of Cr(III) and total Cr remaining in the filtrate was dramatically decreased with this treatment, while the concentration of Cr(VI) remaining was extremely low and did not change significantly.

PANI/SSP has a high ability to remove Cr(VI) under acidic conditions due to the higher reduction potential of polyaniline at these pH values. The ionic equations for the reduction of Cr(VI) to Cr(III) under acidic conditions are as follows:

$$Cr_2O_7^{2-} + 14H^+ + 6e^- \rightarrow 2Cr^{3+} + 7H_2O$$

$$HCrO_4^- + 7H^+ + 3e^- \rightarrow Cr^{3+} + 4H_2O$$

In the pH range of 1–5, increasing pH decreases the content of Cr(III) remaining in the filtrate after the treatment by PANI/SSP. In the pH range of 1–2, Cr(III) was the primary Cr form, and the amount of Cr(VI) in the filtrate was extremely low due to the low adsorption capacity of SSP for Cr(III) at a low pH. Therefore, it is evident that inorganic acid can be used as a desorption solvent for Cr(III). In the pH range of 5–12, the Cr(VI) content in the filtrate increased slowly after treatment with PANI/SSP; the concentration of total Cr remained at extremely low levels due to the higher adsorption capacity for Cr(VI) and Cr(III) in this pH range. In the pH range 12–13, the concentration of Cr(VI) increased remarkably as the reducing capacity of polyaniline decreased significantly. Cr(VI) became the primary form of Cr in the filtrate, some newly reduced Cr(III) was prone to being adsorbed on the surface of SSP, and the rest of this Cr(III) became $Cr(OH)_3$ deposits.

### 3.2. Effect of adsorbent dosage

The dosage of PANI/SSP is a key factor in the detoxification of Cr(VI). The effect of the PANI/SSP dosage on the Cr(VI) removal efficiency from contaminated water is shown in Fig. 1B. The removal percentage of Cr(VI) increased linearly with increasing dosage of PANI/SSP (from 2 to 10 g/L). The removal percentage was 100% for Cr(VI) at a dosage of 8 g/L. The reason for this phenomenon could be that the high PANI/SSP dosage provides more active sites for adsorption of Cr(VI) [14].

### 3.3. Effect of contact time

The effect of contact time on Cr(VI) removal was investigated in the range of 0–60 min. Fig. 1C shows the PANI/SSP Cr(VI) removal efficiencies for different contact times. The adsorption equilibrium was approached within approximately 30 min, which indicates that

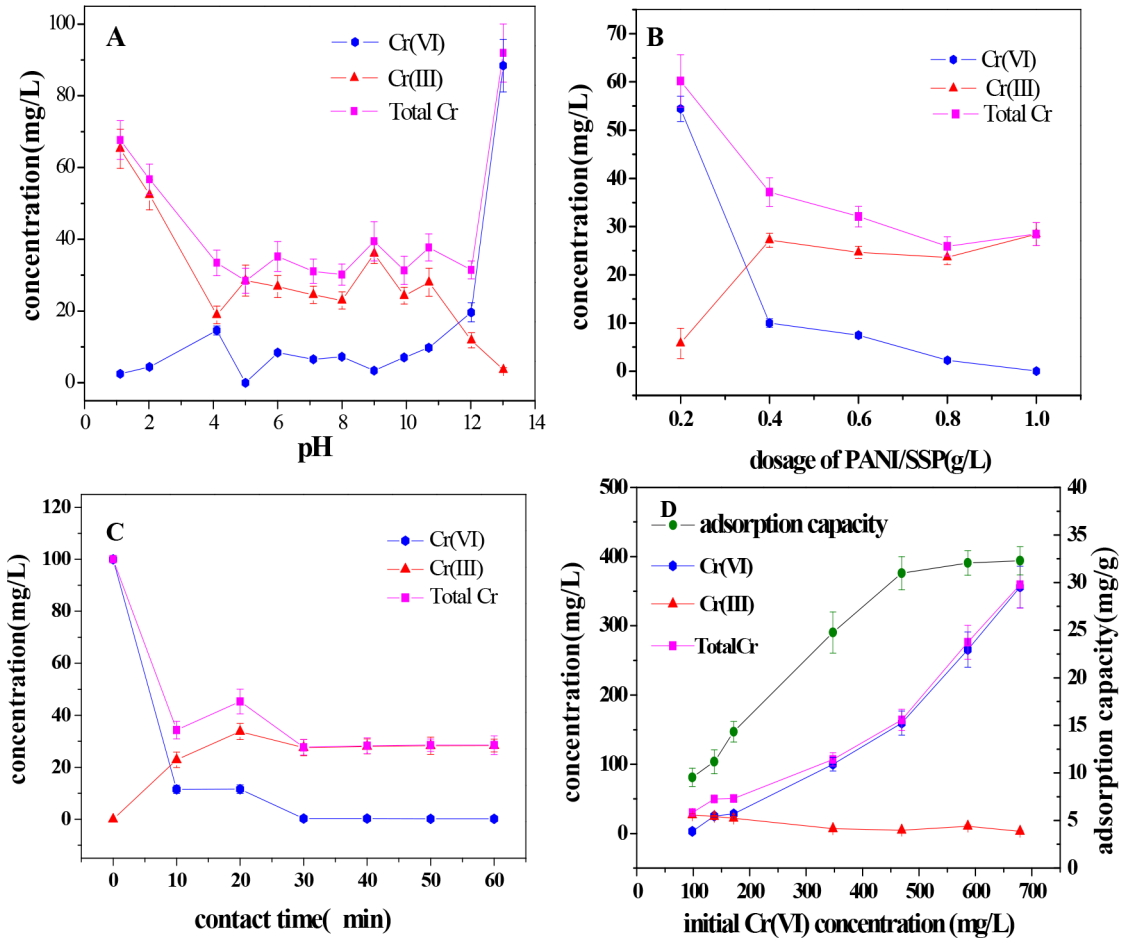


Fig. 1. Effect of operating parameters on Cr(VI), Cr(III), and total Cr concentrations of treated water, (A) Effect of initial pH of Cr(VI)-contaminated water. Initial Cr(VI) concentration of contaminated water, 100 mg/L; dosage of PANI/SSP, 10 g/L; contact time, 1 h; (B) Effect of dosage of PANI/SSP. Initial Cr(VI) concentration of contaminated water, 100 mg/L; solution pH, 4.8; contact time, 1 h; (C) Effect of contact time. Initial Cr(VI) concentration of contaminated water, 100 mg/L; solution pH, 4.8; dosage of PANI/SSP, 10 g/L; (D) Effect of initial Cr(VI) concentration. Contact time, 30 min; solution pH, 4.8; dosage of PANI/SSP, 10 g/L.

the rate of adsorption between PANI/SSP and Cr(VI) is extremely high. The removal rate of Cr(VI) can rise to as much as 90% within the first ten minutes. During the first twenty minutes, the concentration of Cr(III) in the filtrate gradually increased, the concentration maximum value is 33.75 mg/L. As the contact time increased further, the concentration of Cr(III) decreased to approximately 27 mg/L and remained unchanged. These results show that the reaction time between Cr(VI) and the polyaniline deposited on the SSP is negligible, and hence, the adsorption of Cr(III) is the control step in the complete reduction-adsorption of hexavalent chromium by PANI/SSP.

### 3.4. Effect of initial Cr(VI) concentration

With increasing Cr(VI) initial concentration, the mass transfer resistance between the aqueous and solid phases decreases gradually until the reaction equilibrium is reached [15]. In this study, the initial concentration of Cr(VI) was increased from 100 to 700 mg /L. The reaction reached an equilibrium for an initial Cr(VI) concentration of 469 mg/L, and the equilibrated adsorption capacity was approximately 32.10 mg/g. As shown in Fig. 1D, with increasing Cr(VI) initial concentration, the concentration of total Cr and Cr(VI) in the filtrate increased linearly.

Based on these results, we can conclude that the concentration of Cr(III) after adsorption by PANI/SSP under different adsorption conditions is relatively higher than that of other conductive polymer/cellulose fiber composites, except at high concentrations of Cr(VI). Using PANI/SSP as an adsorbent, the concentration of Cr(III) was approximately 25 mg/L in the filtrate, but after treatment with other biomass-based composites such as PPy/CF [16] and PANI/CF [17], the concentration of Cr(III) was negligible. These phenomena may contribute to the low adsorption capacity of SSP for Cr(III) compared with the capacity of pulp fiber. A higher initial concentration of Cr(VI) can effectively overcome all mass transfer resistance because there is a higher probability of collision between Cr(VI) and PANI/SSP. Hence, the concentration of Cr(III) in the filtrate is extremely low at high initial Cr(VI) concentrations.

## 4. Adsorption isotherm and kinetics

### 4.1. Adsorption isotherm

Adsorption isotherms play a vital role in the analysis of the sorption mechanism and surface properties of adsorbent. As shown in Fig. 2A, isotherms describe the relation between the $q_e$ and equilibrium concentration ($C_e$) at a fixed temperature. The experimental data were fitted to a series of isotherm models such as the Langmuir, Freundlich, and Temkin models using Origin 8.0 software. The fitted results and linear forms of these isotherm models are presented in Table 1.

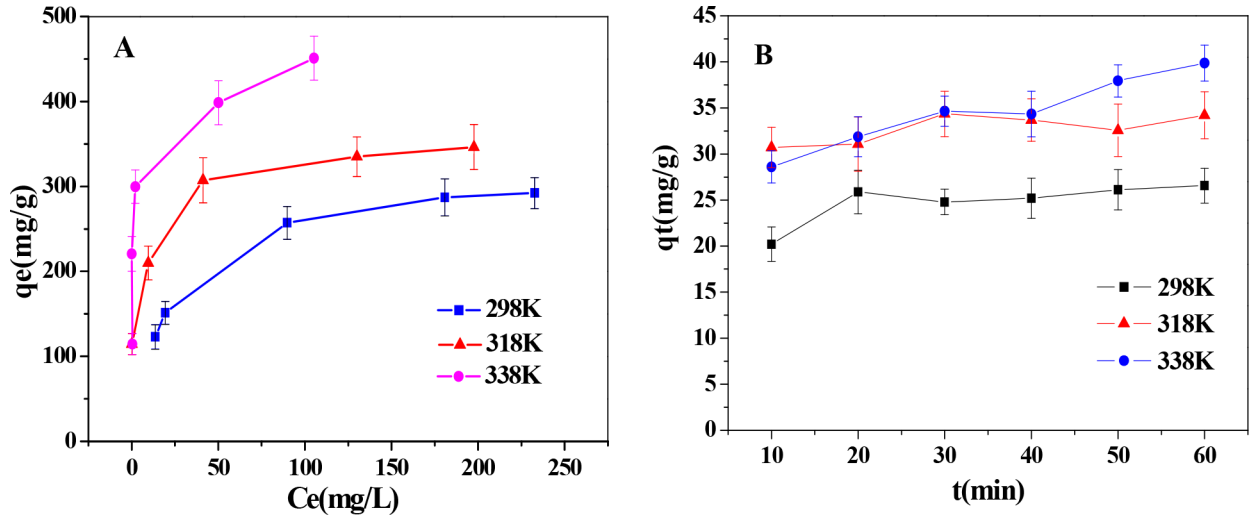


Fig. 2. Equilibrium isotherms and kinetic data of Cr(VI) adsorption onto PANI/SSP at different temperature.

Table 1
Isotherm parameters for Cr(VI) adsorption onto PANI/SSP

| Isotherm model | | Parameter | $R^2$ | Equation | Linear forms |
|---|---|---|---|---|---|
| Langmuir | 298K | $q_m$ = 32.05 mg/g<br>$b$ = 0.0458 L/mg<br>$R_L$ = 0.0399–0.138 | 1 | $q_e = C_e/(0.0312\ C_e + 0.681)$ | |
| | 318K | $q_m$ = 35.09 mg/g<br>$b$ = 0.232 L/mg<br>$R_L$ = 0.00786–0.0362 | 0.9987 | $q_e = C_e/(0.0285\ C_e + 0.123)$ | $\frac{C_e}{q_e} = \frac{1}{q_m b} + \frac{C_e}{q_m}$ |
| | 338K | $q_m$ = 44.84 mg/g<br>$b$ = 0.609 L/mg<br>$R_L$ = 0.00290–0.0140 | 0.9955 | $q_e = C_e/(0.0223\ C_e + 0.0366)$ | |
| Freundlich | 298K | $K$ = 5.88 mg/g<br>$n$ = 3.268 | 0.9597 | $\ln q_e = 0.306 \ln C_e + 1.772$ | |
| | 318K | $K$ = 14.86 mg/g<br>$n$ = 5.917 | 0.9798 | $\ln q_e = 0.169 \ln C_e + 2.700$ | $\ln q_e = \ln K + \frac{\ln C_e}{n}$ |
| | 338K | $K$ = 22.09 mg/g<br>$n$ = 6.667 | 0.5268 | $\ln q_e = 0.150 \ln C_e + 3.095$ | |
| Temkin | 298K | $A$ = –3.149<br>$B$ = 6.118 | 0.9835 | $q_e = -3.149 + 6.118\ C_e$ | |
| | 318K | $A$ = 15.894<br>$B$ = 3.549 | 0.9591 | $q_e = 15.894 + 3.549\ C_e$ | $q_e = A + B\ln C_e$ |
| | 338K | $A$ = 24.430<br>$B$ = 4.126 | 0.7389 | $q_e = 24.430 + 4.126\ C_e$ | |

The concrete explanations for the bases of these isotherm models has been discussed in several previous reports; therefore, we do not provide their elaboration here. Based on the $R^2$ values (see Table 1), the order of the fitting quality using the isothermal adsorption models is as follows: Langmuir > Temkin > Freundlich.

Based on the fit to the data by the Langmuir isotherm model, in the temperature range from 298 K to 338 K with an increase in adsorption, the minimum and maximum adsorption capacities were 31.13 mg/g and 45.07 mg/g, respectively. The capacity of Cr(VI) adsorption onto PANI/SSP was compared with that of the other adsorbents reported in the literature and is tabulated in Table 2. The boiled sunflower stem and head had a relatively low adsorption capacity for Cr(VI) (4.9 mg/L and 7.9 mg/L, respectively). The capacity of PANI/SSP for Cr(VI) adsorption is more than six times that of sunflower stem. In addition, we can combine the biomass with a conductive polymer to effectively improve the adsorption capacity of biomass for Cr(VI). Compared with other conductive polymer/biomass hybrids, PANI/SSP has several advantages such as low cost, easy availability of raw materials, and a wide pH response range.

The *b* value increased slightly with increasing temperature, which indicates that a high temperature is beneficial for the adsorption of Cr(VI). The effect of the adsorption temperature on Cr(VI) removal will be analyzed in the thermodynamic section in detail. The $R_L$ values were less than 1 at the different temperatures, which suggests that this adsorbent can easily adsorb Cr(VI) and has better ability to treat Cr(VI) [24]. Hence, we conclude that the PANI/SSP has valuable potential for the detoxification of Cr(VI) from sewage.

Table 2
Adsorption capacity of different adsorbents for hexavalent chromium

| Adsorbents | Adsorption capacity (mg/g) | Ref. |
|---|---|---|
| Boiled sunflower stem | 4.9 | [18] |
| Boiled sunflower head | 7.9 | [19] |
| PANI/ Filter-Paper | 31.72 | [20] |
| PANI/Kapok | 44.05 | [21] |
| PPy/Natural corncob-core sponge | 84.7 | [22] |
| PPy/Chitosan | 78.61 | [23] |
| PANI/SSP | 31.13 | Present work |

### 4.2. Adsorption kinetics

The study of adsorption kinetics is vital for the evaluation of the adsorption efficiency and mechanism. The adsorption kinetics reveals the variation in the instantaneous absorption capacity with adsorption time. The effect of temperature on the kinetic behavior of adsorption was investigated at different temperatures (illustrated in Fig. 2B). To determine the optimal kinetic model, the experimental data were fitted with pseudo first order, pseudo second order, and Elovich models. The fitting results are presented in Table 3.

The coefficient of determination ($R^2$) for the pseudo second order kinetic model is greater than that for the pseudo first order and Elovich kinetic models. Thus, the kinetics of Cr(VI) adsorption using PANI/SSP as an adsorbent can be better explained by the pseudo second order kinetic model. In addition, the equilibrium adsorption capacity ($q_{e,cal}$) determined from the pseudo second order model was closer to the experimental value ($q_{e,exp}$), further demonstrating that the pseudo second order model can effectively describe the adsorption of Cr(VI). The $q_e$ increases with increasing adsorption temperature. These results suggest that the adsorption of Cr(VI) onto PANI/SSP is an endothermic process, which is consistent with the thermodynamic analysis.

## 5. Thermodynamic parameters

The relationship between the Gibbs free energy and the thermodynamic equilibrium constant

$$K_a = \frac{q_e}{C_e} \tag{3}$$

is well known and can be expressed via the following two equations:

$$\Delta G^o = -RT \ln K_a \tag{4}$$

$$\Delta G^o = \Delta H^o - T\Delta S^o \tag{5}$$

where $R$ is a thermodynamic constant (R≈8.314 J/mol·K), T is the adsorbent temperature, $\Delta H^o$ is the standard enthalpy change, and $\Delta S^o$ is the standard entropy change. The adsorption thermodynamic equation

$$\ln K_a = \frac{\Delta S^o}{R} - \frac{\Delta H^o}{RT} \tag{6}$$

Table 3
Kinetics parameters for Cr(VI) adsorption onto the PANI/SSP

| | | Pseudo-first-order | | | Pseudo-second-order | | | Elovich | | |
|---|---|---|---|---|---|---|---|---|---|---|
| Temperature (K) | $q_{e\,exp}$ (mg/g) | $k_1$ (1/min) | $q_{e1\,cal}$ (mg/g) | $R^2$ | $k_2$ (g/mg·min) | $q_{e2\,cal}$ (mg/g) | $R^2$ | α (mg/g·min) | β (g/mg) | $R^2$ |
| 298 | 27.12 | 0.03825 | 6.38 | 0.6185 | 0.0117 | 27.73 | 0.9968 | 371.4965 | 0.3313 | 0.6645 |
| 318 | 35.36 | 0.02218 | 4.73 | 0.2437 | 0.0209 | 34.54 | 0.9959 | 244903.8275 | 0.5345 | 0.5127 |
| 338 | 40.57 | 0.05064 | 25.77 | 0.8056 | 0.0035 | 42.96 | 0.9870 | 68.1372 | 0.1692 | 0.9144 |

can be derived from Eqs. (4) and (5). The values of $\Delta H^o$ and $\Delta S^o$ for the adsorption process can be determined from the slope and intercept of the plot of $ln\ K_a$ vs. $1/T$ (data not provided). The thermodynamic parameters calculated by the above method for the adsorption of Cr(VI) onto PANI/SSP at different temperatures are tabulated in Table 4.

The positive values of Gibb's free energy change prove the nonspontaneous nature of adsorption. The positive entropy change suggests increased randomness at the solid/solution interface during the adsorption of Cr(VI) onto PANI/SSP. The enthalpy change was positive, showing that the adsorption of Cr(VI) is endothermic [25].

## 6. Fourier transform infrared analysis (ATR-FTIR)

The ATR-FTIR spectra of bare SSP, PANI/SSP, and PANI/SSP loaded with Cr(VI) are shown in Figs. 3A–C. In bare SSP, the characteristic peaks at 3411 $cm^{-1}$ are indicative of the presence of hydroxide radicals, which can form intermolecular hydrogen bonds. The additional peak at 2926 $cm^{-1}$ can be assigned to the C-H stretching. The adsorption peaks at approximately 1630 $cm^{-1}$, 1538 $cm^{-1}$, and 1425 $cm^{-1}$ are assigned to the characteristic peaks of the aromatic hydrocarbon skeleton. The additional peaks at 1739 $cm^{-1}$ and 1060 $cm^{-1}$ are assigned to C=O and C-O stretching, respectively. Unsaturated C-H out-of-plane bending was observed at 727 $cm^{-1}$. These results provide evidence of the presence of hydroxide radicals, carboxylic groups, intermolecular hydrogen bonds, and aromatic compounds in the SSP. As shown in Fig. 3B, the characteristic peaks of polyaniline were observed at 1588 $cm^{-1}$, 1495 $cm^{-1}$, 1308 $cm^{-1}$, and 1049 $cm^{-1}$, namely, the C=C stretching vibration in the quinone ring of polyaniline at 1495 $cm^{-1}$, the characteristic peaks of the benzene ring at 1588 $cm^{-1}$, the C-H bending vibration at 1049 $cm^{-1}$, the C-N stretching vibrations at 1308 $cm^{-1}$, and the C-H bending vibration peak outside of the aromatic ring plane at 803 $cm^{-1}$. After the modification of SSP, the intensity of the hydroxyl stretching vibration at 3418 $cm^{-1}$ was clearly reduced, because the surface hydroxide radical of the SSP was coated with polyaniline. The above results are related to the presence of polyaniline on the surface of SSP. As shown in Fig. 3C, the characteristic peaks of polyaniline shift to 1591 $cm^{-1}$, 1498 $cm^{-1}$, 1313 $cm^{-1}$, and 1059 $cm^{-1}$ when the SSP was loaded with Cr(VI). This phenomenon confirms that the polyaniline was oxidized by hexavalent chromium.

Table 4
Thermodynamic parameters for Cr(VI) uptake by the PANI/SSP

| Temperature (K) | Thermodynamic parameters | | | |
|---|---|---|---|---|
| | $\Delta G^0$ (KJ/mol) | $\Delta S^0$ (KJ/mol·K) | $\Delta H^0$ (KJ/mol) | $R^2$ |
| 298 | 4.7788 | | | |
| 308 | 3.6848 | | | |
| 318 | 2.5908 | 0.1094 | 37.38 | 0.9974 |
| 328 | 1.4968 | | | |
| 338 | 0.4028 | | | |

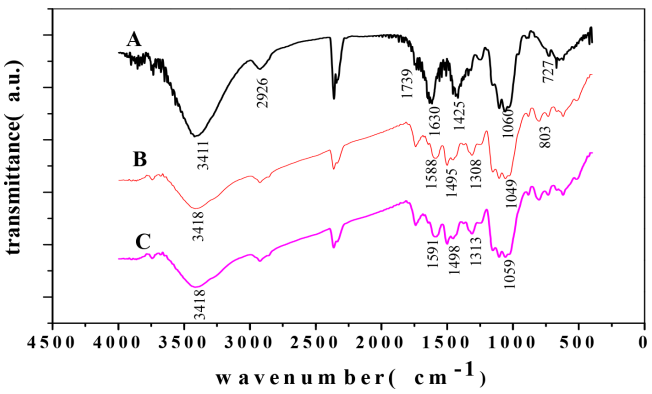


Fig. 3. ATR-FTIR spectra of (A) SSP, (B) PANI/SSP and (C) PANI/SSP adsorbed with Cr(VI).

## 7. SEM and TEM

The surface morphology of the SSP and PANI/SSP before and after adsorption Cr(VI) was investigated by SEM and TEM, as shown in Fig. 4 and Fig. 5. The surface of SSP presented a pseudohexagonal multipore structure with a relatively smooth surface (Fig. 4A and Fig. 5A), while the SEM micro graphs suggest that PANI/SSP had an irregular porous honeycomb structure with a high specific surface area. After in situ polymerization, granular polyaniline was formed, and then a part of the polyaniline was well distributed on the surface of the SSP (Fig. 4B and Fig. $4B_1$). Another part of the approximately 12 nm polyaniline granule spread to the internal holes of the SSP (Fig. $5B_1$)

However, the deposition rate of the polyaniline was extremely low (approximately 11.4%), as polyaniline does not completely cover the surface of the SSP (Fig. 4B). The surface morphology of PANI/SSP before and after adsorption Cr(VI) do not clearly differ (Fig. 4C and Fig. $4C_1$), as the hexavalent chromium is present as ions.

## 8. TG and DTG analysis

The thermal stability of the PANI/SSP was analyzed from the TG and DTG data taken at a heating rate of 10°C/min. As shown in Fig. 6, the thermal degradation can be divided into two stages. The first stage occurred in the range of 220–300°C and involved approximately 10% loss in weight; the peak temperature for the maximum decomposition of PANI/SSP was 230°C. These results are probably due to the degradation of hemicellulose [26]. The second stage occurred in the range of 300–350°C and involved a weight loss of 25% for PANI/SSP; the peak temperature for maximum decomposition was 322°C. These results can primarily be explained by the degradation of cellulose and polyaniline [26,27]. The total weight loss was approximately 35% in the range from 30°C–550°C, which indicates that the PANI/SSP has great thermal stability.

## 9. Regeneration study

The recycling and regeneration of the PANI/SSP are crucial for future practical applications. The regeneration efficiency of the PANI/SSP was estimated by performing

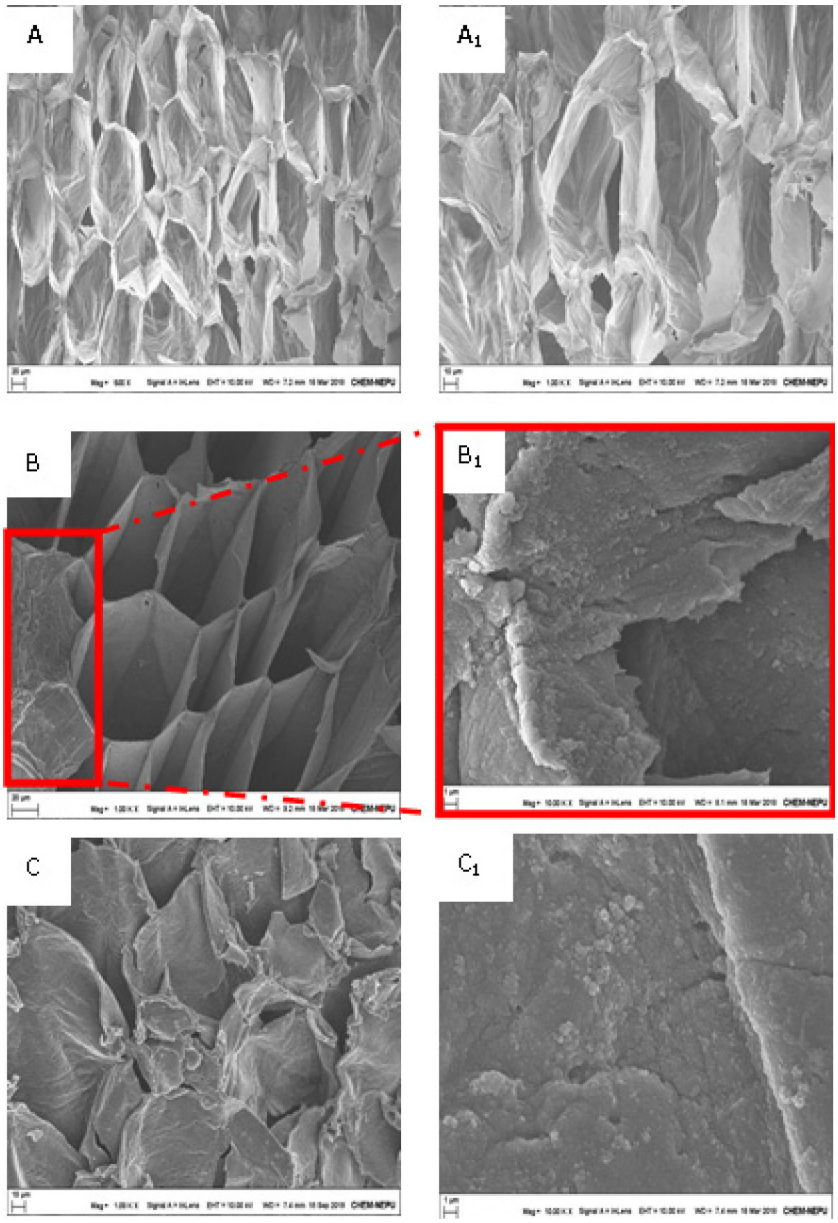


Fig. 4. Scanning electron microscopic images of (A) SSP (500×), ($A_1$) SSP (1000×), (B) PANI/SSP (1000×), ($B_1$) PANI/SSP (10000×), (C) PANI/SSP adsorbed with Cr(VI) (1000×), ($C_1$) PANI/SSP adsorbed with Cr(VI) (10000×).

adsorption-desorption experiments for five cycles. The results are shown in Fig. 7. The removal efficiency was 79.56% after five cycles. Hence, the PANI/SSP can be successively reused for four adsorption-desorption cycles without any loss of Cr(VI) removal capacity. These results provide evidence that PANI/SSP is excellent for the detoxification of Cr(VI).

## 10. Adsorption mechanism

The BET surface area and porous properties of the PANI/SSP were determined from $N_2$ adsorption-desorption experiments (Table 5). As per the nitrogen adsorption-desorption analysis, the BET surface area and Barret-Joyner-Halenda (BJH) desorption cumulative pore volume of PANI/SSP were measured as 2.60 $m^2/g$ and 0.01 $cm^3/g$, respectively, which are higher than those of SSP (2.24 $m^2/g$ and 0.0047 $cm^3/g$, respectively). The pore size of PANI/SSP was 25.26 nm, which is much larger than that of SSP (18.15 nm), indicating the mesoporous character of the PANI/SSP. This phenomenon primarily occurs because the oxidant (APS) and dopant (HCl) promote the hydrolysis of cellulose during the preparation of PANI/SSP.

The nitrogen adsorption-desorption isotherms of PANI/SSP and SSP are shown in Fig. 8. The data exhibit a typical type-I adsorption-desorption isotherm curve (Langmuir isotherm) with a hysteresis loop according to IUPAC classifications.

To confirm the adsorption mechanism of Cr(VI), XPS was used to investigate the surface elemental composition of the

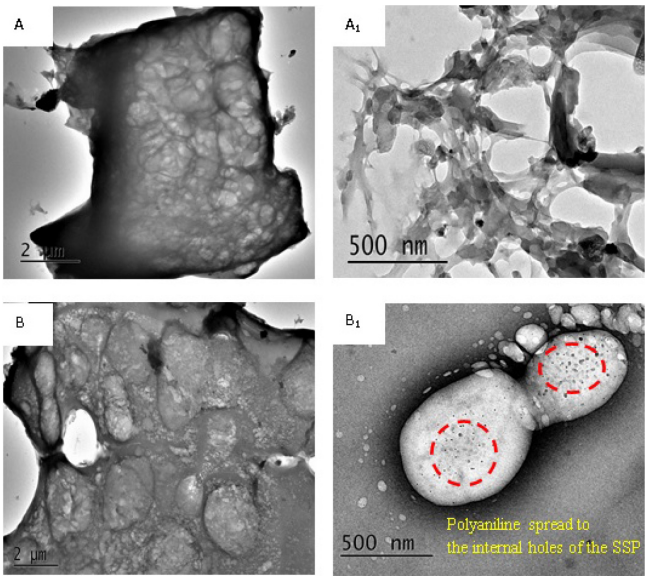


Fig. 5. Transmission electron microscopes images of SSP (A and $A_1$) and PANI/SSP (B and $B_1$).

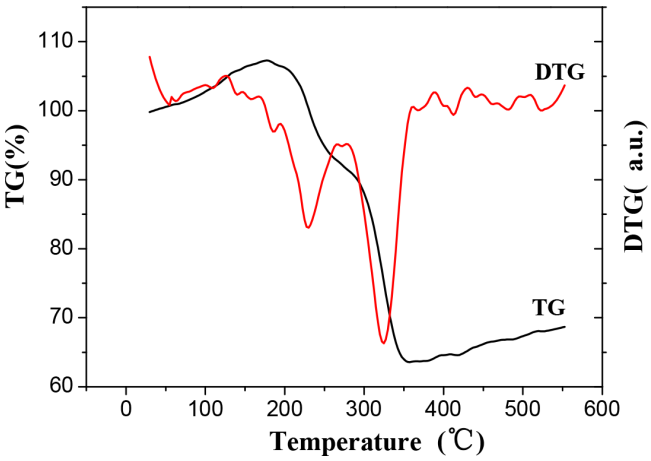


Fig. 6. TG and DTG curve of PANI/SSP.

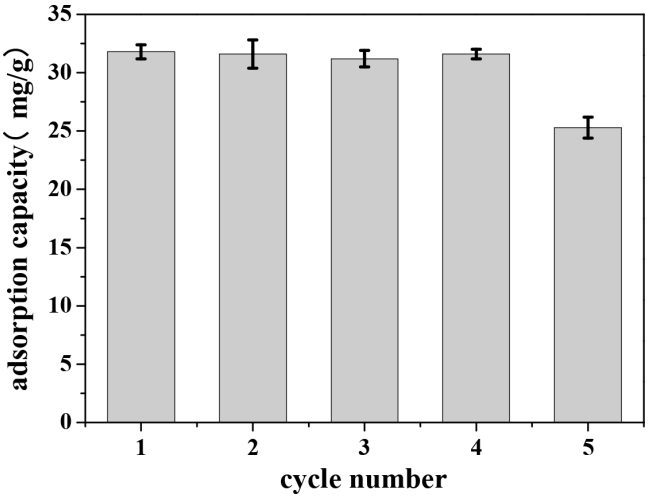


Fig. 7. Adsorption-desorption cycles. Adsorption condition: Cr(VI) concentration of contaminated water, 500 mg/L; dosage of PANI/SSP, 10 g/L; contact time, 6 h; pH of Cr(VI)-contaminated water, 4.8.

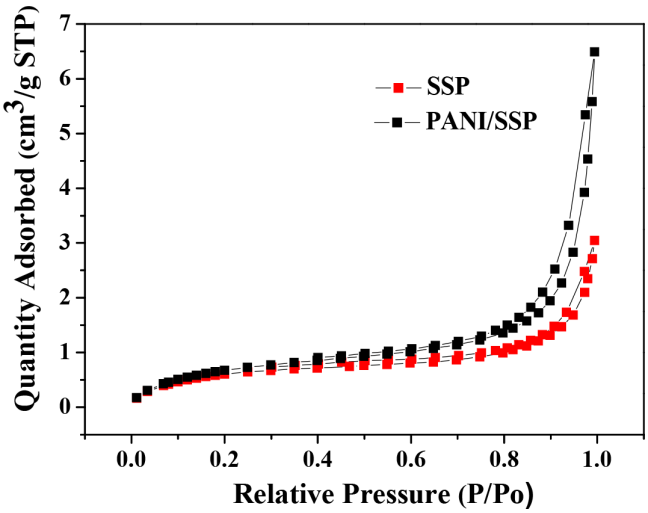


Fig. 8. Nitrogen adsorption/desorption isotherms for SSP and PANI/SSP.

PANI/SSP before and after adsorption of Cr(VI). The results are illustrated in Fig. 9A and Fig. 9B. The binding energies of 575.8 eV and 585.98 eV refer to Cr 2p3/2 and Cr 2p1/2 spin-orbit peaks, respectively [28]. These results suggest that both Cr(VI) and Cr(III) are present on the surface of PANI/SSP.

On the one hand, Cr(VI) was reduced to Cr(III) by polyaniline, and then Cr was adsorbed on the surface of negatively charged PANI/SSP. On the other hand, Cr(VI) exchanged ions with chloride ions that were doped on the polyaniline molecules. Hence, the adsorption mechanism of Cr(VI) was reduction-coupled adsorption and ion exchange. The fraction of Cr(VI) and Cr(III) as a percent of the total Cr on the surface of PANI/SSP after adsorption were calculated to be 58.97% and 41.02%, respectively. The content of Cr(III) was relatively low due to the relatively poor adsorption of Cr(III). As illustrated in Fig. 1, more Cr(III) was present in the filtrate after the detoxification of Cr(VI) than before detoxification.

The N1s spectrum of PANI/SSP before the adsorption of Cr(VI) can be deconvoluted into three peaks (Fig. 9C);

Table 5
Surface properties of the PANI/SSP before and after adsorption for Cr(VI)

| Adsorbents | Surface area (SBET)/($m^2$/g) | Pore size(BJH)/nm | Pore volume/($cm^3$/g) |
|---|---|---|---|
| SSP | 2.24 $m^2$/g | 18.15 | 0.0047 |
| PANI/SSP | 2.60 $m^2$/g | 25.26 | 0.01 |

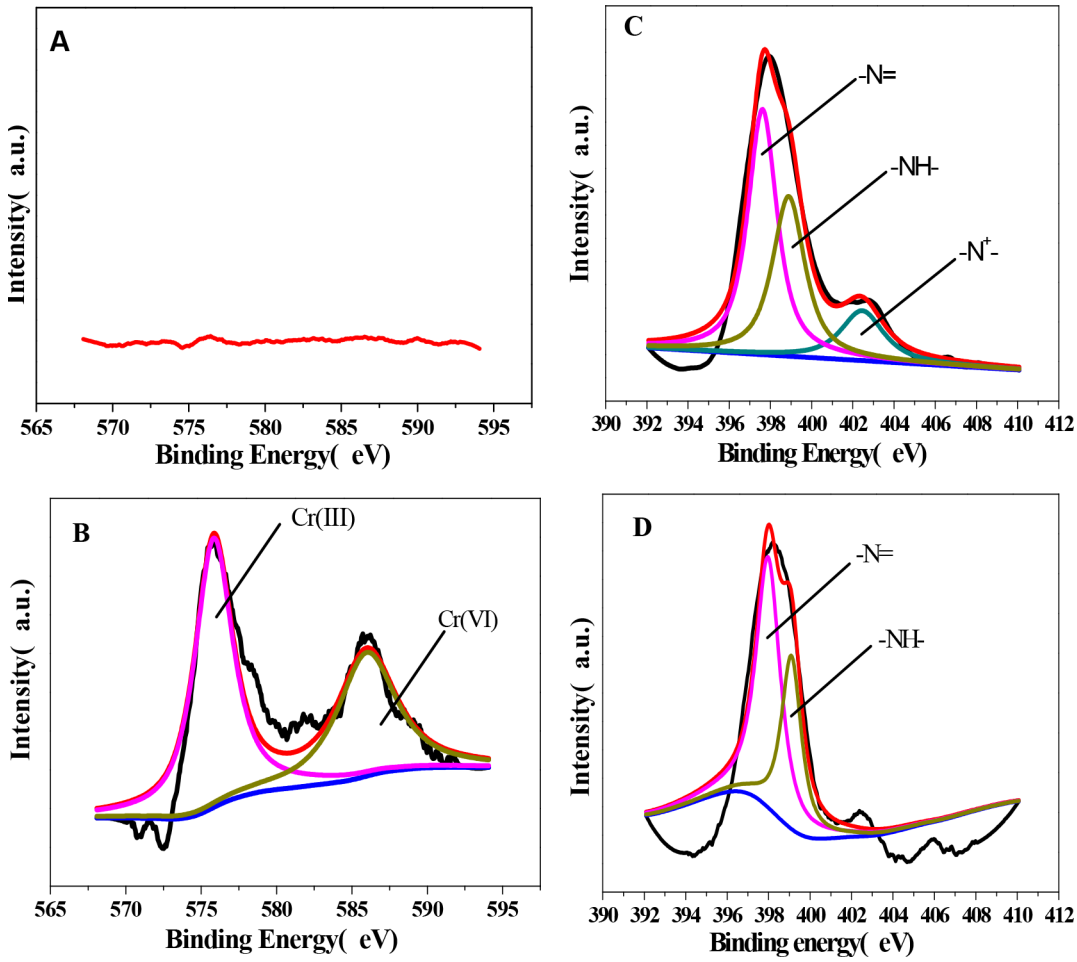


Fig. 9. Cr2p3/2 and N 1s core level spectra of PANI/SSP before(A and C) and after Cr(VI) adsorption(B and D).

the peak at 397.5 eV is related to the quinoid imine (–N=), the peak at 399.7 eV represents benzenoid amine (–NH), and the peak at 402.5 eV represents the protonated amine (–$N^+$–). The percentage of quinoid imine (–N=) increased from 49.90% to 63.34% as almost all the protonated amine (–$N^+$–) was converted into quinoid imine (–N=) during adsorption (Table 6 and Fig. 9D). This change primarily occurred because the reduction of Cr(VI) requires protons and electrons from a protonated amine.

## 11. Conclusion

This study focused on the detoxification of Cr(VI)-contaminated water using PANI/SSP as an adsorbent. PANI/SSP exhibited a wide pH response range; in the pH range of 5–11, when the initial concentration of Cr(VI) was 100 mg/L, the removal rate of Cr(VI) was more than 90%. The adsorption isotherm results suggested that the adsorption process can be described by a Langmuir isotherm with a maximum adsorption capacity of 42.96 mg/g at 338 K. The experimental data were well fit with the pseudo second order kinetic model, and the thermodynamic analysis demonstrated that the adsorption of Cr(VI) onto PANI/SSP is endothermic. The TG-DTG analysis showed that PANI/SSP has high thermal stability. XPS studies suggested that the adsorption mechanism of Cr(VI) was reduction-coupled adsorption and ion exchange. Overall, this study demonstrated that PANI/SSP is an effective and inexpensive adsorbent for the detoxification of Cr(VI) from contaminated water.

Table 6
Cr1S and N1 s XPS deconvolution results of the PANI/SSP before and after adsorption for Cr(VI)

| Sample | Cr1s | | N1s | | |
|---|---|---|---|---|---|
| | Cr(2p3/2) 575.83eV | Cr(2p1/2) 585.9eV | –N= 397.5eV | –N–H– 399.7eV | –$N^+$–402.5eV |
| Before adsorption | 0 | 0 | 49.49 | 35.81 | 14.70 |
| After adsorption | 58.97 | 41.02 | 63.34 | 36.66 | 0 |

**Acknowledgement**

The authors gratefully acknowledge the National Natural Science Foundation of China (Grant No. 21507009), National Foundation for Studying Abroad (Grant No. 留金亚[2016]9082), NEPU Scientific Research Foundation (rc201726) Natural Science and Foundation of Heilongjiang Province (B2016002) for financial support to this work.

**References**

[1] A. Saravanan, P.S. Kumar, M. Yashwanthra, Sequestration of toxic Cr(VI) ions from industrial wastewater using waste biomass: A review, Desal. Water Treat., 68 (2017) 245–266.
[2] V. Sarin, K.K. Pant, Removal of chromium from industrial waste by using eucalyptus bark, Bioresour. Technol., 97(1) (2006) 15–20.
[3] M. Bhaumik, H.J. Choi, M.P. Seopela, R.I. McCrindle, A. Maity, Highly effective removal of toxic Cr(VI) from wastewater using sulfuric acid-modified avocado seed, Ind. Eng. Chem. Res., 53(3) (2014) 1214–1224.
[4] M. Jain, V.K. Garg, K. Kadirvelu, Chromium(VI) removal from aqueous system using Helianthus annuus (sunflower) stem waste, J. Hazard. Mater., 162(1) (2009) 365–372.
[5] M. Jain, V.K. Garg, K. Kadirvelu, Equilibrium and kinetic studies for sequestration of Cr(VI) from simulated wastewater using sunflower waste biomass, J. Hazard. Mater., 171(1–3) (2009) 328–334.
[6] Y.S. Shen, S.L. Wang, S.T. Huang, Y.M. Tzou, J.H. Huang, Biosorption of Cr(VI) by coconut coir: Spectroscopic investigation on the reaction mechanism of Cr(VI) with lignocellulosic material, J. Hazard. Mater., 179(1–3) (2010) 160–165.
[7] Z.G. Ng, J.W. Lim, M.H. Isa, V.R. Pasupuleti, N.M. Yunus, K.C. Lee, Adsorptive removal of hexavalent chromium using sawdust: Enhancement of biosorption and bioreduction, Sep. Sci. Technol., 52(10) (2017) 1707–1716.
[8] N.A. Manikandan, A.K. Alemu, L. Goswami, K. Pakshirajan, G. Pugazhenthi, Waste litchi peels for Cr(VI) removal from synthetic wastewater in batch and continuous systems: sorbent characterization, regeneration and reuse study, J. Environ. Eng., 142(9) (2016) C4016001.
[9] L. Tang, Y. Fang, Y. Pang, G. Zeng, J. Wang, Y. Zhou, Y. Deng, G. Yang, Y. Cai, J. Chen, Synergistic adsorption and reduction of hexavalent chromium using highly uniform polyaniline–magnetic mesoporous silica composite, Chem. Eng. J., 254 (2014) 302–312.
[10] G. Yang, L. Tang, Y. Cai, G. Zeng, P. Guo, G. Chen, Y. Zhou, J. Tang, J. Chen, W. Xiong, Effective removal of Cr(VI) through adsorption and reduction by magnetic mesoporous carbon incorporated with polyaniline, RSC Adv., 4(102) (2014) 58362–58371.
[11] Y. Zheng, W. Wang, D. Huang, A. Wang, Kapok fiber oriented-polyaniline nanofibers for efficient Cr(VI) removal, Chem. Eng. J., 191 (2012) 154–161.
[12] X. Liu, X. Qian, J. Shen, W. Zhou, X. An, An integrated approach for Cr(VI)-detoxification with polyaniline/cellulose fiber composite prepared using hydrogen peroxide as oxidant, Bioresour. Technol., 124 (2012) 516–519.
[13] R. Ansari, N.K. Fahim, Application of polypyrrole coated on wood sawdust for removal of Cr(VI) ion from aqueous solutions, React. Funct. Polym., 67(4) (2007) 367–374.
[14] J.C.P. Vaghetti, E.C. Lima, B. Royer, J.L. Brasil, B.M. da Cunha, N.M. Simon, N.F. Cardoso, C.P.Z. Noreña, Application of Brazilian-pine fruit coat as a biosorbent to removal of Cr(VI) from aqueous solution—Kinetics and equilibrium study, Biochem. Eng. J., 42(1) (2008) 67–76.
[15] Y. Khambhaty, K. Mody, S. Basha, B. Jha, Biosorption of Cr(VI) onto marine Aspergillus niger: experimental studies and pseudo-second order kinetics, World J. Microbiol. Biotechnol., 25(8) (2009) 1413–1421.
[16] Y. Lei, X. Qian, J. Shen, X. An, A process of applying polypyrrole-engineered pulp fibers prepared using hydrogen peroxide as oxidant to detoxification of Cr(VI)-contaminated water, Bioresour. Technol., 131 (2013) 134–138.
[17] X. Liu, W. Zhou, X. Qian, J. Shen, X. An, Polyaniline/cellulose fiber composite prepared using persulfate as oxidant for Cr(VI)-detoxification, Carbohydr. Polym., 92(1) (2013) 659–661.
[18] M. Jain, V.K. Garg, K. Kadirvelu, Chromium(VI) removal from aqueous system using Helianthus annuus (sunflower) stem waste, J. Hazard. Mater., 162(1) (2009) 365–372.
[19] M. Jain, V.K. Garg, K. Kadirvelu, Equilibrium and kinetic studies for sequestration of Cr(VI) from simulated wastewater using sunflower waste biomass, J. Hazard. Mater., 171 (2009) 328–334.
[20] X. Li, W. Liu, M. Li, Y. Li, M. Ge, Characterizations and Cr (VI) adsorption properties of polyaniline/filter-paper composite, Polym. Comp., 35(5) (2014) 993–998.
[21] Y. Zheng, W. Wang, D. Huang, A. Wang, Kapok fiber oriented-polyaniline nanofibers for efficient Cr(VI) removal, Chem. Eng. J., 191 (2012) 154–161.
[22] J. Zhang, H. Chen, Z. Chen, J. He, W. Shi, D. Liu, H. Chi, F. Cui, W. Wang, Micro structured macro porous adsorbent composed of polypyrrole modified natural corncob-core sponge for Cr(VI) removal, RSC Adv., 6(64) (2016) 59292–59298.
[23] R. Karthik, S. Meenakshi, Removal of hexavalent chromium ions from aqueous solution using chitosan/polypyrrole composite, Desal. Water Treat., 56(6) (2014) 1587–1600.
[24] C. Namasivayam, D. Kavitha, Removal of congo red from water by adsorption onto activated carbon prepared from coir pith, an agricultural solid waste, Dyes Pigm., 54(1) (2002) 47–58.
[25] B. Singha, S.K. Das, Biosorption of Cr(VI) ions from aqueous solutions: kinetics, equilibrium, thermodynamics and desorption studies, Colloids Surf. B Biointerf., 84(1) (2011) 221–232.
[26] S.A. El-Sayed, M.E. Mostafa, Pyrolysis characteristics and kinetic parameters determination of biomass fuel powders by differential thermal gravimetric analysis (TGA/DTG), Energy Convers. Manage., 85 (2014) 165–172.
[27] S.X. Wang, L.X. Sun, Z.C. Tan, F. Xu, Y.S. Li, Synthesis, characterization and thermal analysis of polyaniline(pani)/$Co_3O_4$ composites, J. Therm. Anal. Calorim., 89(2) (2007) 609–612.
[28] Y. Lei, X. Qian, J. Shen, X. An, Integrated reductive/adsorptive detoxification of Cr(VI)-contaminated water by polypyrrole/cellulose fiber composite, Ind. Eng. Chem. Res., 51(31) (2012) 10408–10415.